

# Effect of Matrix's Type on the Dynamic Properties for Short Fiber-Elastomer Composite

MICHIO ASHIDA and TORU NOGUCHI, *Department of Industrial Chemistry, Faculty of Engineering, Kobe University, Nada, Kobe 657, Japan*, and SATOSHI MASHIMO, *Mitsuboshi Belting Ltd., Nagata, Kobe 653, Japan*

## Synopsis

The dynamic moduli,  $E'$  and  $E''$ , and  $\tan \delta$  for PET-CR, PET-EPDM, and PET-UR composites with unidirectional short fibers were studied as a function of temperature by using a Rheovibron. The temperature dependence of  $\tan \delta$  showed three peaks for PET-elastomer composites. The peaks at the low temperature corresponded to the main dispersion of the respective matrixes and the peak at about 140°C to the  $\alpha$ -dispersion of PET fiber. A small and broad peak observed at a temperature between 60 and 120°C may be caused by the relaxation of the interface region between fibers and matrix. The longitudinal storage modulus for the composite  $E'_l$  was given by the parallel model as  $E'_l = V_f \cdot E'_f + V_m \cdot E'_m$  where  $E'_f$  and  $E'_m$  are the storage moduli for fiber and matrix and  $V_f$  and  $V_m$  are the volume fraction of fiber and matrix, respectively. In the transverse direction of fibers, the composite modulus  $E'_t$  was expressed by the logarithmic law of mixing as follows:  $\log E'_t = V_f \cdot \log E'_f + V_m \cdot \log E'_m$ . The peak values of  $\tan \delta$  from the main dispersion of the respective matrixes were given by the equation,  $(\tan \delta_{1, \max})_c / (\tan \delta_{\max})_m = 1 - \beta \cdot V_f$ , where  $(\tan \delta_{1, \max})_c$  and  $(\tan \delta_{\max})_m$  are the maximum values of the loss tangent for the composite and matrix, respectively, and  $\beta$  is coefficient depending on matrix's type. The  $\beta$  value of PET-CR composite is the largest one among those of the composites.

## INTRODUCTION

Short fiber-elastomer composites are interesting and useful materials possessing both the flexibility of elastomer and the stiffness of fiber. The mechanical properties of the composites, such as modulus, strength, and ultimate elongation, depend on fiber orientation, fiber aspect ratio, and adhesion between fiber and matrix.<sup>1-7</sup> In previous articles,<sup>8-10</sup> the authors reported the adhesive effect on the mechanical properties and swelling behavior for PET-CR, nylon-CR, PET-UR, and PET-EPDM composites. It was found that PET and nylon fibers oriented well along the flow direction in rubber compound during roll process and that these composites showed the anisotropy for the mechanical properties and swelling. The stress-strain curves for the composites with untreated fibers showed that PET-CR composite was yielded by a stress of approximately 10 MPa and extended over a large portion of the strain range and that the PET-EPDM composite was yielded at the half stress of that of CR composite. When short fibers were treated with RFL bonding agent, the tensile stress of these composites increased sharply with increasing strain and they had very high modulus and low elongation at the break point. For PET-UR composite, on the contrary, the tensile stress of the composite including fibers which were

treated by isocyanate increased gradually as well as one including untreated fibers with increasing strain.

The dynamic moduli,  $E'$  and  $E''$ , and the mechanical damping,  $\tan \delta$ , for nylon-CR and PET-CR composites with unidirectional short fibers have been investigated as a function of temperature by a Rheovibron.<sup>11,12</sup> In the longitudinal direction of fibers, the storage moduli for nylon-CR and PET-CR composites were given by the parallel model. The temperature dependence of  $\tan \delta$  for these composites showed two dispersion peaks corresponding to the components. The peak at  $-28^\circ\text{C}$  corresponded to the main dispersion of CR and another peak at higher temperature to the  $\alpha$ -dispersion of loaded fibers. In addition, a small and broad peak was observed at about  $90^\circ\text{C}$ . This peak may be caused by the interface region in the composite. The interface between fibers and matrix seems to play an important role on the mechanical properties of short fiber-elastomer composites. Lees,<sup>13</sup> Derringer,<sup>14</sup> and Halpin<sup>15,16</sup> have proposed some equations regarding the moduli of elastomers filled with short fibers. However, any of earlier investigations have not referred to the change of the properties caused by the interface between fibers and matrix.

In this study, in order to investigate the effect of fiber addition to some elastomers, the short fiber-elastomer composites are prepared with three kinds of elastomer and PET fiber. The elastomers used are CR, EPDM, and UR, because CR has polar chains, EPDM is a nonpolar polymer, and the UR composite can be composed without carbon black. The effect of elastomer types on the dynamic viscoelasticity and the mechanism of the reinforcement for these composites are investigated.

### EXPERIMENTAL

The short fiber used was PET of  $21 \mu\text{m}$  in diameter and 6 mm in length (Teijin Co., Ltd.). CR (Denka Co., Ltd.), EPDM (Mitsui Petrochemical Industries, Ltd.), and Urethan rubber (UR, Bayer AG) were used as elastomer. The recipe of rubber compound are given in Table I. In order to increase their adhesion to elastomer matrix as CR and EPDM, PET fibers were dipped in isocyanate solution and then treated with RFL bonding agent as described in the previous article.<sup>11</sup> In the case of PET-UR composite, PET fibers were treated only with isocyanate solution.

TABLE I  
Compound Recipe (phr)

Ingredient	CR	EPDM	UR
Matrix rubber	100	100	100
Carbon black	36	45	—
Process oil	4	4	—
Stearic acid	2	1	0.5
Antioxidant	2	—	—
MgO	4	—	—
ZnO	5	5	—
Ethylene thiourea	0.5	—	—
Accelerator	—	3	1
Sulfur	—	1	—
DCP	—	—	3
PET	a	a	a

<sup>a</sup> Variable.

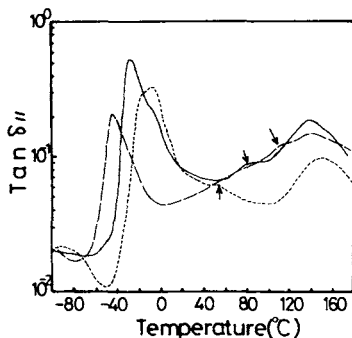


Fig. 1. Temperature dependence of  $\tan \delta_{||}$  at 11 Hz for composites: (—) PET-CR; (— —) PET-EPDM; (- - -) PET-UR. Arrows show the additional dispersions.

The unidirectional short fiber-elastomer composites were prepared by the same procedure of mixing and vulcanization as described in the previous article.<sup>11</sup> The cured specimens of 2 mm in thickness were cut out in a long plate of  $10 \times 70$  mm along the longitudinal direction or the transverse direction of fibers.

The dynamic complex modulus  $E^*$  and  $\tan \delta$  of the specimens were measured along both the longitudinal direction ( $\parallel$ ) and the transverse direction ( $\perp$ ) of fibers by a direct reading dynamic viscoelastometer Rheovibron Model DDV-III (Toyo Baldwin Co., Ltd.). The temperature range over which the properties were determined was  $-100$ – $160^\circ\text{C}$  at a heating rate of  $1^\circ\text{C}/\text{min}$ , at frequencies of 3.5, 11, 35, and 110 Hz with a strain amplitude of 0.06–0.1%.

## RESULTS AND DISCUSSION

The temperature dependence of  $\tan \delta_{||}$  for PET-CR, PET-EPDM, and PET-UR composites is shown in Figure 1. Large peaks observed at temperatures of  $-40$ ,  $-28$ , and  $-15^\circ\text{C}$  correspond to the main dispersions of EPDM, CR, and UR matrix, respectively. A moderate peak observed at about  $140^\circ\text{C}$  for all the composites arises from the  $\alpha$ -dispersion of PET fiber. In addition, a small and broad peak is observed at a temperature between the two peaks, as is shown with arrows. When  $\tan \delta$  is measured in the transverse direction of fibers, this peak of  $\tan \delta_{\perp}$  becomes larger and more distinct, as is shown in Figure 2. These additional dispersions are observed

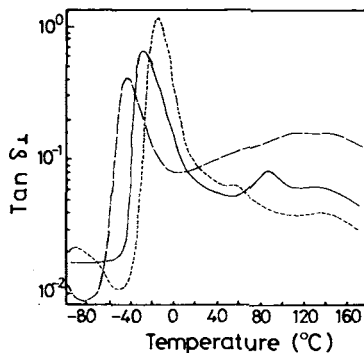


Fig. 2. Temperature dependence of  $\tan \delta_{\perp}$  at 11 Hz for composites: (—) PET-CR; (— —) PET-EPDM; (- - -) PET-UR.

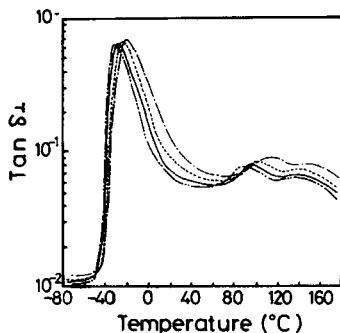


Fig. 3. Effect of frequency on temperature dependence of  $\tan \delta_1$  for PET-CR composite. The frequencies are 3.5 Hz (---), 11 Hz (—), 35 Hz (---), and 110 Hz (-·-·-).

at temperatures of 60°C, 90°C, and 120°C for PET-UR, PET-CR, and PET-EPDM composites, respectively. These dispersions show the different shapes individually and the magnitude of  $\tan \delta$  peak for PET-UR composite is small comparing with those for other composites. Figure 3 shows the effect of measuring frequency on  $\tan \delta_1$  for the PET-CR composite. The peak of  $\tan \delta_1$  corresponding to the main dispersion of CR shifts to the higher temperature by 7°C as the frequency increases to tenfold. For the peak at about 90°C, the shift to high temperature is larger than that of the main dispersion of CR. Shifts in the peak of loss moduli for the composites depended on the frequency similar to the peak temperature of  $\tan \delta$ . Figure 4 shows the relationship between the peak temperature and the frequency for the individual dispersion peaks of PET-CR composite. Based on the linear relationship, the apparent activation energy  $H$  of a dispersion is given by the following equation:

$$\log f = \log f_0 - H/2.303 \cdot RT \quad (1)$$

where  $f_0$  is an experimental constant,  $f$  and  $T$  are the measuring frequency and temperature for the dispersion peak, respectively, and  $R$  is a gas constant. The activation energies of each dispersion for these composites are obtained by this way and summarized in Table II. In the case of PET-UR composite, the activation energy for the main dispersion of matrix was nearly equal to that of UR alone. For PET-EPDM composite, the activation

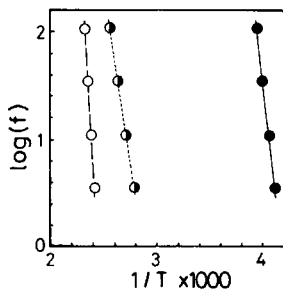


Fig. 4. Relationship between frequency and peak temperature of dispersions for PET-CR composite: main dispersion of CR (●), additional dispersion (◐), and  $\alpha$ -dispersion of PET fiber (○).

TABLE II  
Activation Energy of Individual Dispersion

CR	Matrix		Fiber, PET
	EPDM	UR	
151	105	159	314 (kJ/mol)
Composites	Main dispersion of matrix <sup>a</sup>	$\alpha$ -Dispersion of PET fiber <sup>b</sup>	Additional dispersion <sup>a</sup>
PET-CR	251	310	130
PET-EPDM	126	335	126
PET-UR	163	318	151

<sup>a</sup> Transverse direction of fibers.

<sup>b</sup> Longitudinal direction of fibers.

energy was slightly larger than that of EPDM alone. In the case of PET-CR composite, on the contrary, the activation energy of the main dispersion of matrix was  $250 \text{ kJ} \cdot \text{mol}^{-1}$ , which was considerably larger than the value of CR alone. The results suggest that the UR matrix in the PET-UR composite holds its original properties probably owing to poor adhesion and that the mobility of CR matrix in the composite is confined by good adhesion of PET fibers. For all the composites, the activation energy of the  $\alpha$ -dispersion of PET fiber was about  $320 \text{ kJ} \cdot \text{mol}^{-1}$ , which was nearly equal to the value of PET fiber. In the case of additional dispersion, the activation energies are about  $130 \text{ kJ} \cdot \text{mol}^{-1}$  for all the composites and the values close to that of the respective elastomer matrix alone. Because this dispersion was not observed in the composites filled with untreated PET fibers, this dispersion may be attributed to the new phase, which is formed at the interface between matrix and fibers treated with the bonding agent.

The microbrownian motion of elastomer matrix is frozen at the temperature under  $T_g$  of matrix. Figure 5 shows the dynamic storage moduli at  $-80^\circ\text{C}$  as a function of the volume fraction of PET fiber for PET-CR, PET-EPDM, and PET-UR composites. The values of  $E'_1$  for these composites increase almost linearly with increasing  $V_f$ , as is shown in the solid lines. The intercepts of these lines coincide with the  $E'$  value of the respective

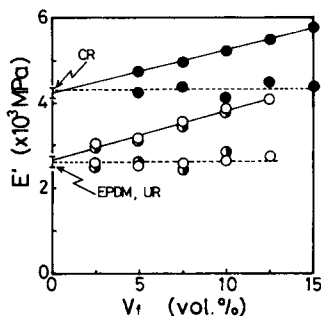


Fig. 5. Effect of fiber loading on the dynamic storage moduli,  $E'_1$  (—) and  $E'$  (- - -), at  $-80^\circ\text{C}$  for composites: (●) PET-CR; (○) PET-EPDM; (◐) PET-UR. Arrows show the  $E'$  values of the respective matrices.

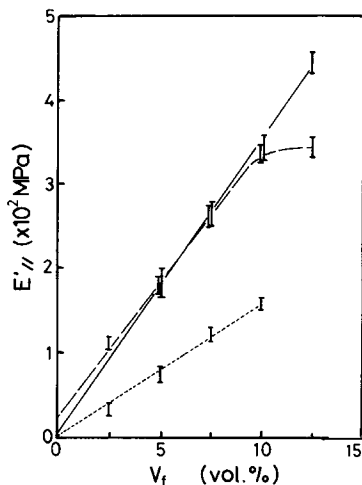


Fig. 6. Effect of fiber loading on the longitudinal storage moduli  $E'_//$  at 20°C for composites: (—) PET-CR; (---) PET-EPDM; (- - -) PET-UR.

elastomer matrix, and the slopes of them are nearly parallel to each other. The values of  $E'_//$  for each composite take the ones of the respective matrix independent of fiber's volume fraction. Figure 6 shows the effect of the volume fraction of fiber on  $E'_//$  at 20°C for PET-CR, PET-EPDM, and PET-UR composites. The values of  $E'_//$  increase linearly with increasing fiber loading except that of PET-EPDM composite containing 12.5 vol % of the fiber. From the figure, the slopes and the intercepts of the individual lines drawn through the points of  $E'_//$  are given in Table III. As reported previously,<sup>11</sup> in the longitudinal direction of fibers the dynamic storage moduli for nylon-CR and PET-CR composites were given by the parallel model as follows:

$$E'_// = V_f \cdot E'_f + V_m \cdot E'_m = (E'_f - E'_m) \cdot V_f + E'_m \quad (2)$$

where  $E'_f$  and  $E'_m$  are the dynamic storage moduli for fiber and elastomer matrix, and  $V_f$  and  $V_m$  are the volume fraction of them, respectively. The moduli for fiber and matrix obtained at 20°C are also given in Table III. In the case of PET-CR and PET-EPDM composites, it was found that the moduli at 20°C agree nearly with the values calculated from the parallel model. This "parallel model" based on the assumption that matrix and

TABLE III  
Factor of Fiber Loading for the Longitudinal Composite Moduli of Short  
Fiber-Elastomer Composites

Composite	Observed		Parallel Model	
	Slope (MPa)	Intercept (MPa)	$E'_f - E'_m$ (MPa)	$E'_m$ (MPa)
PET-CR	3500	3.3	3750	13.8
PET-EPDM	3200	26.4	3740	20.0
PET-UR	1800	2.4	3760	4.5

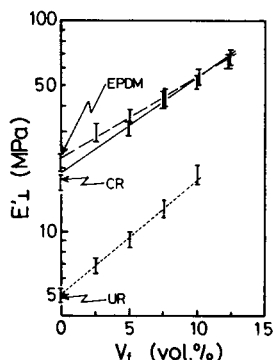


Fig. 7. Effect of fiber loading on the transverse storage moduli  $E'_1$  at 20°C for composites: (—) PET-CR; (---) PET-EPDM; (· · ·) PET-UR. Arrows show the  $E'$  values of the respective matrices.

fibers were strained to the same extent.<sup>17</sup> The finding suggests that the fibers bond strongly to the matrix so that the fiber strain equals to the matrix's one in the range of the tensile strain, which is applied to the composite by the viscoelastometer, and that eq. (2) can be applied well to these composites. In the case of PET-UR composite, however, the observed slope is about one half of the value of that calculated from the parallel model. As described in the previous paper,<sup>10</sup> although the PET fibers in the PET-UR composite took very high orientation similar to other composites, the tensile stress was smaller than those of PET-EPDM and PET-CR composites. The finding suggests that UR matrix adheres poorly to PET fibers. The  $E'_1$  values at 20°C are plotted on the logarithmic axis against the volume fraction of fiber for these composites, as is shown in Figure 7. The  $\log E'_1$  values increase linearly with increasing  $V_f$ , and the obtained  $E'_1$  values are much larger than those calculated from the modified Halpin-Tsai equation for the transverse composite moduli.<sup>18,19</sup> The value of  $\log E'_1$  is expressed as the following equation:

$$\log E'_1 = a + b \cdot V_f \quad (3)$$

where  $a$  and  $b$  are constants. The values of  $a$  and  $b$  are obtained from the intercepts and the slopes in Figure 7, respectively. In order to compare with the bonding force of PET fiber to matrix, the  $a$  and  $b$  values of untreated PET-elastomer composites are obtained in the same way and are listed in Table IV. It is well known that the modulus for many composites consisted of two phases can be expressed by "the logarithmic law of mixing" as follows<sup>20</sup>:

$$\begin{aligned} \log E'_c &= V_m \cdot \log E'_m + V_f \cdot \log E'_f \\ &= \log E'_m + V_f \cdot \log E'_f/E'_m \end{aligned} \quad (4)$$

where the subscripts  $c$ ,  $m$ , and  $f$  denote composite, matrix, and fiber, respectively. The values of  $a$  and  $b$  in eq. (3) correspond to  $\log E'_m$  and  $\log E'_f/E'_m$  in eq. (4), respectively. As is shown in Table IV, the values of  $a$  agree

TABLE IV  
Factor of Fiber Loading for the Transverse Composite Moduli of Short Fiber-Elastomer Composites

Composite	Observed			Logarithmic law of mixing		
	Intercept ( $\alpha$ )	Slope ( $b$ )	$\log E'_m$	$\log E'_f/E'_m$	$b/\log E'_f/E'_m$	$b/\log E'_f/E'_m$
PET-CR	Treatment <sup>a</sup>	3.99	1.15	2.46	1.62	1.62
	Nontreatment	2.63	1.15	2.46	1.07	1.07
PET-EFDM	Treatment <sup>a</sup>	3.49	1.30	2.27	1.54	1.54
	Nontreatment	2.60	1.30	2.27	1.15	1.15
PET-UR	Treatment <sup>b</sup>	3.43	0.65	2.92	1.17	1.17
	Nontreatment	3.12	0.65	2.92	1.07	1.07

<sup>a</sup> RFL treatment.

<sup>b</sup> Isocyanate treatment.



with  $\log E'_m$  for all composites. Since the values of  $b$  for the composites with untreated PET fibers are nearly equal to the values of  $\log E'_f/E'_m$ , eq. (4) can be applied well to the transverse storage moduli of these composites. In the case of treated PET fibers, the  $b$  values obtained are much larger than the values of  $\log E'_f/E'_m$ . When the ratio of  $b$  to  $\log E'_f/E'_m$  is given by  $\gamma$ ,  $b$  is expressed as follows:

$$b = \gamma \cdot \log E'_f/E'_m$$

By putting these values into eq. (3), we obtain

$$\log E'_1 = \log E'_m + \gamma \cdot V_f \cdot \log E'_f/E'_m \quad (5)$$

where the  $\gamma$  value is a factor indicating the degree of the bonding force between fibers and matrix. That is, the  $\gamma$  value is unity when the fiber is untreated and increases with increasing the bonding force. In other words, the apparent volume fraction of fiber,  $V'_f (= \gamma \cdot V_f)$ , becomes larger than the true volume fraction of fiber with increasing adhesion.<sup>19-21</sup> The modulus of particle filled-elastomer composite was given by "the logarithmic law of mixing"<sup>22</sup> or the modified one.<sup>23</sup> Gray and McCrum<sup>24</sup> indicated that the modulus of polymers consisted of the crystalline region and the amorphous one was also given by eq. (4). Therefore, it seems that short fibers in the transverse direction act just like particles or crystalline regions to reinforce matrix.

As described in the previous article,<sup>11</sup> the maximum values of  $\tan \delta$  for the main dispersion of elastomer matrix decreased linearly with increasing  $V_f$  and the intercepts of the lines agreed with  $\tan \delta_{\max}$  values of matrix alone. Consequently, the values of  $\tan \delta_{1\max}$  are given as

$$(\tan \delta_{1\max})_c = (\tan \delta_{\max})_m - \alpha \cdot V_f$$

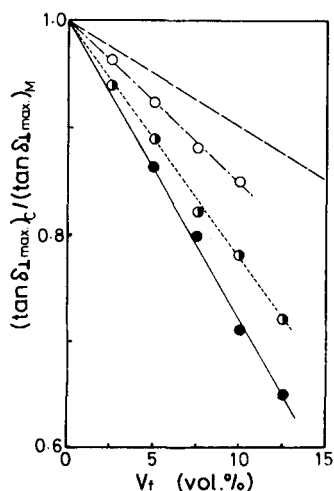


Fig. 8. Effect of fiber loading on the maximum values of  $\tan \delta_1$  at the main dispersion of the respective matrixes for composites: (●) PET-CR; (◐) PET-EPDM; (○) PET-UR. (— —) Value calculated from eq. (6) when the  $\beta$  value is unity.

TABLE V  
Interaction Coefficient and S-S Properties in the Longitudinal Direction of Fibers for PET  
Fiber-Elastomer Composites

Composite	Surface treatment on PET	$\beta$	10% tensile stress (MPa)	Tensile strength (MPa)
PET-CR	Treatment <sup>a</sup>	3.0	11.3	20.2
	Nontreatment	2.2	11.0	13.1
PET-EPDM	Treatment <sup>a</sup>	2.2	8.7	13.4
	Nontreatment	1.8	5.6	7.6
PET-UR	Treatment <sup>b</sup>	1.5	6.8	13.2
	Nontreatment	1.3	6.3	12.3

<sup>a</sup> RFL treatment.

<sup>b</sup> Isocyanate treatment.

that is,

$$(\tan \delta_{1\max})_c / (\tan \delta_{\max})_m = 1 - \beta \cdot V_f \quad (6)$$

where  $\beta$  is a coefficient depending on the matrix. From the value of  $\beta$  in eq. (6), the degree of the interaction between fibers and matrix can be estimated. Figure 8 shows the effect of fiber loading on the relative damping,  $(\tan \delta_{1\max})_c / (\tan \delta_{\max})_m$ , for the composites. If the mechanical damping comes only from the matrix polymer, the relative damping is roughly equal to the volume fraction of matrix<sup>24,25</sup> and decrease along the dash line, as is shown in Figure 8. The values of the composites decrease along more steeper lines with increasing fiber loading. The values of  $\beta$  in eq. (6) are obtained from the slopes of these lines in Figure 8 and are shown in Table V. In the case of untreated PET-elastomer composite, the value of  $\beta$  for nonpolar EPDM-composite is smaller than that of polar CR-composite. The value of PET-UR composite is the smallest among the PET-elastomer composites, and there is no noticeable increase of  $\beta$  value after the isocyanate treatment on PET fibers. On the other hand, the  $\beta$  values for CR and EPDM composites increase considerably by using the treated PET fiber and the  $\beta$  value of PET-CR composite increases larger than that of PET-EPDM composite. When the  $\beta$  value is much larger than unity, the region with strong interaction is formed at the interface between fibers and matrix, and decrease the apparent volume fraction of matrix.<sup>19-27</sup> The additional dispersion for treated PET-elastomer composites may be caused by the relaxation of this interface region in the composites.

The shapes of stress-strain curves for both PET-CR and PET-EPDM composites are quite similar to each other, as described in the previous article.<sup>10</sup> The tensile stress at 10% extension and the tensile strength for the respective composites are also shown in Table V. Comparing the  $\beta$  values with the mechanical properties, it is found that the tensile stress and the tensile strength are comparable with the  $\beta$  values for these composites. Therefore, for short fiber-elastomer composites, their mechanical properties at large deformation would be able to be predicted from the dynamic properties at very small strain.

## References

1. A. Y. Coran, K. Boustany, and P. Hamed, *Rubber Chem. Technol.*, **47**, 396 (1974).
2. A. Y. Coran, K. Boustany, and P. Hamed, *J. Appl. Polym. Sci.*, **15**, 2471 (1971).
3. A. Y. Coran, P. Hamed, and L. A. Goetter, *Rubber Chem. Technol.*, **49**, 1167 (1976).
4. S. R. Moghe, *Rubber Chem. Technol.*, **47**, 1074 (1974).
5. S. R. Moghe, *Rubber Chem. Technol.*, **49**, 1160 (1976).
6. J. E. O'Connor, *Rubber Chem. Technol.*, **50**, 945 (1977).
7. A. P. Foldi, *Rubber Chem. Technol.*, **49**, 379 (1976).
8. T. Noguchi, M. Ashida, and S. Mashimo, *Nippon Gomu Kyokaishi*, **56**, 768 (1983).
9. T. Noguchi, M. Ashida, and S. Mashimo, *Nippon Gomu Kyokaishi*, **57**, 171 (1984).
10. T. Noguchi, M. Ashida, and S. Mashimo, *Nippon Gomu Kyokaishi*, **57**, 744 (1984).
11. M. Ashida, T. Noguchi, and S. Mashimo, *J. Appl. Polym. Sci.*, **29**, 661 (1984).
12. M. Ashida, T. Noguchi, and S. Mashimo, *J. Appl. Polym. Sci.*, to appear.
13. J. K. Lees, *Polym. Eng. Sci.*, **8**, 186 (1968).
14. G. C. Derringer, *J. Elastoplast.*, **3**, 230 (1971).
15. J. C. Halpin, *J. Compos. Mater.*, **3**, 732 (1969).
16. J. C. Halpin and J. L. Kardos, *J. Appl. Phys.*, **43**, 2235 (1972).
17. B. C. Blackley and N. T. Pike, *Kautschuk Gummi Kunststoff*, **29**, 680 (1976).
18. L. E. Nielsen, *J. Appl. Phys.*, **41**, 4626 (1970).
19. T. B. Lewis and L. E. Nielsen, *J. Appl. Polym. Sci.*, **14**, 1449 (1970).
20. L. E. Nielsen, *Mechanical Properties of Polymers and Composites*, Marcel Dekker, New York, 1975.
21. K. D. Ziegel, *J. Colloid Interface Sci.*, **29**, 72 (1969).
22. K. Fujimoto and T. Nishi, *Nippon Gomu Kyokaishi*, **43**, 54 (1970).
23. S. Nohara, *Kobunshi Kagaku*, **28**, 527 (1955).
24. R. W. Gray and N. G. McCrum, *J. Polym. Sci.*, A-2, **7**, 1329 (1969).
25. B. L. Lee and L. E. Nielsen, *J. Polym. Sci.*, *Polym. Phys. Ed.*, **15**, 683 (1977).
26. L. E. Nielsen, *J. Polym. Sci.*, *Polym. Phys. Ed.*, **17**, 1897 (1979).
27. I. Souma, *J. Appl. Polym. Sci.*, **27**, 1523 (1982).

Received March 7, 1984

Accepted June 21, 1984

Corrected proofs received December 13, 1984.